NASA TN D-204

7N-07
197736
40P

TECHNICAL NOTE

D-204

EXPERIMENTAL DETERMINATION OF THE TEMPERATURE AND DYNAMIC-STRAIN ENVIRONMENT OF A TUBULAR COMBUSTOR LINER IN A TURBOJET ENGINE

By Patrick T. Chiarito, William C. Morgan, and C. Robert Morse

Lewis Research Center
Cleveland, Ohio

NATIONAL AERONAUTICS AND SPACE ADMINISTRATION

WASHINGTON March 1960

NATIONAL AERONAUTICS AND SPACE ADMINISTRATION

TECHNICAL NOTE D-204

EXPERIMENTAL DETERMINATION OF THE TEMPERATURE AND DYNAMIC-STRAIN ENVIRONMENT OF A TUBULAR COMBUSTOR LINER IN A TURBOJET ENGINE

By Patrick T. Chiarito, William C. Morgan, and C. Robert Morse

SUMMARY

Cracking of combustor liners results from a complex of loads imposed during engine operation. This investigation was made to supply information on environmental factors that must be understood before the failure mechanism can be identified. Metal temperatures, vibratory frequencies, and dynamic strains were measured.

The results of this study indicate that the temperature of the sheet-metal liner was not influenced appreciably by hot starts or shutdown procedure. The maximum thermal gradient was 1500° F per inch and was measured near a cooling louver at rated speed.

The range of vibratory frequencies measured was between 4000 and 10,500 cycles per second at all strain-gage locations. These excitations were attributed to the last five compressor rotor stages. It appears that mechanical fatigue could contribute measurably to cracking, especially at louvers. Although the maximum dynamic-stress range measured was only 5400 psi, peak dynamic stresses might exceed the endurance limit of the sheet material during the service life of the liner.

INTRODUCTION

Service records of turbojet engines show frequent cracking of combustor liners (ref. 1). The cracks generally originate at geometrical discontinuities such as cooling louvers or air-intake holes and propagate to adjacent louvers or holes. Early replacement of the liners usually results. Occasionally, a piece of the liner may break away and pass through the turbine with additional damage ensuing.

Relatively little information appears in the literature regarding analysis of the cause of the cracking, although frequent mention is made of the possibility of thermal fatigue resulting from repeated starts, transients, and shutdowns (ref. 2). In addition, relatively little information regarding the temperature and the stress environment of the sheet-metal combustor during engine operation is available. Metal temperatures measured in the combustor of a J33 turbojet were reported (ref. 3), but no data were found for temperatures in other tubular combustors or for vibratory strains in the thin sheet-metal liners for any type of engine.

This investigation was made to obtain a better understanding of the causes of cracking in tubular combustor liners by measuring the metal temperatures, vibratory frequencies, and dynamic strain in the sheet-metal walls during engine operation. The following information was desired: (1) metal temperatures around geometrical discontinuities, (2) the range of frequencies over which the liners are susceptible to vibration, (3) the sources of excitation, and (4) dynamic-stress values near regions where failures usually occur.

A J47-27 engine was chosen for this investigation because the tubular combustor liner was considered to be typical. Operating conditions were varied from start to rated speed and back to shutdown. Temperature histories were obtained for normal and hot starts, and for normal accelerations to rated speed and decelerations to shutdown. The dynamic-strain measurements were limited to slow accelerations, however, to allow the resonant vibrations to build up to maximum amplitudes. This was done to aid in the determination of the order and source of the excitations and not as a means of simulating normal operation.

REMARKS ON GENERAL STRESS STATE IN LINER

The combustor liner used in this investigation is essentially a thin sheet-metal cylinder with one end open and with multiple cutouts to accommodate the flow of cooling air and secondary-combustion air. During engine operation the liner is subjected to a combination of static and dynamic loads that result in the following stresses. All of these stresses are aggravated by stress corrosion and stress concentrations at the edges of the cutouts:

(1) Static-pressure stress

(2) Dynamic stress resulting from mechanical excitation

(3) Dynamic stress resulting from gas forces

(4) Thermal stress resulting from steady-state conditions

(5) Thermal stress resulting from transient conditions

E-387

(6) Residual stress resulting from fabrication process or from plastic flow in prior cycles

Some comments on each of these stresses follow:

(1) Previous unpublished measurements have shown that the maximum pressure drop across the combustor liner is about 4 pounds per square inch (or 5 percent of the sea-level static pressure at military takeoff of approximately 75 lb/sq in. abs at the inlet to the combustor). The compressive hoop stress that would result from this load in a cylinder without cutouts and of the same dimensions (nominal radius of $3\frac{3}{4}$ in. and thickness of 0.040 in.) is approximately 375 psi. Although this stress is relatively small, it is only one of the several factors contributing to the total stress.

(2) The rotating parts of the engine induce mechanical vibrations. When the frequencies match the natural modes of vibration of the liner, resonance will occur and amplitudes may become appreciable (as will the stresses).

(3) Previous research (refs. 4 and 5) has shown that the major source of vibration excitation in compressor and turbine rotor blades is the dynamic gas loading, and it was anticipated that vibration in the liner would also result from the same cause. Considerable research on flat-plate vibration (ref. 6) indicates the complexity of the nodal patterns. Vibration of a curved plate is even more complex, and nothing has been found in the literature on any experiments to isolate the modes of vibration. When cutouts are added to a cylinder, the problem is not conducive to analysis.

(4) Because thermal stress is dependent on both temperature distribution and restraint against expansion, the evaluation of this stress is quite difficult in a complex structure such as a combustor liner. At best, thermal gradient (and its persistence) can be taken as an indication of the possible thermal stress that would result.

(5) Although peak thermal stresses usually result from transient engine operating conditions and are short-lived, the cyclic nature of these stresses is conducive to fatigue-type failures. Frequent mention of thermal fatigue failure appears in the literature.

(6) The air-intake holes and cooling louvers are punched into the sheet metal, and residual stresses are induced. The magnitude of these stresses depends on the sharpness of the tool. A sharp tool will produce clean edges and small residual stresses, whereas a worn tool will cause burrs and large residual stresses.

In addition to the effects of stress corrosion and stress concentrations, additional complexity results from the fact that fuel nozzles often produce nonuniform spray patterns. A previous extensive survey (ref. 1) indicated that hot spots in the liner walls are frequently caused by faulty fuel nozzles. These hot spots are even more common in ignition chambers because of the greater tendency toward carbon deposits, which interfere further with the fuel spray pattern.

An attempt has been made to emphasize the complexity of the loading on a combustor and the need for a better understanding of each factor that contributes to the total stress state. The failure mechanism cannot be well identified until all of the environmental factors are understood. This investigation attempts to supply some of this much-needed information.

APPARATUS

Test Facility

The J47-27 turbojet engine was operated in a static sea-level test stand. The metal-temperature survey was made on one combustor and the strain survey on another combustor. These combustors did not have igniters. Only one instrumented liner was installed at a time because the engine operating procedures for the temperature and strain surveys were quite different (see TEST PROCEDURE, p. 6).

Paint for preliminary measurements. - Several liners were coated with a temperature-sensitive paint for making a general survey of metal temperatures. This paint is originally red and undergoes a clear-cut change in color at the following nominal temperatures ($^{\circ}$F): 770 (brown), 915 (yellow), 1065 (orange), and 1470 (green).

Thermocouples. - Final measurements of metal temperatures were sensed by Chromel-Alumel thermocouples on the outside of the liner, as shown in figure 1(a). The beads were attached by gas welding. Expansion loops were formed in the thermocouple wires between the weld and the end of the Inconel conduit because the exposed wire was broken in previous tests when no loops were used. The end of the conduit was secured to the liner by several straps to reduce the effects of vibration. This method of attachment greatly reduced the number of thermocouple failures, compared with the preliminary tests without expansion loops. Details of the locations of the thermocouples near air-intake holes and cooling louvers at approximately midlength and near the air-intake holes at the downstream end of the liner are shown in figure 1(b).

The exhaust-gas temperature was sensed by 14 Chromel-Alumel thermocouples located 2 inches radially inward from the tailpipe wall and equally spaced around the tailpipe immediately downstream of the tailcone.

Because of the transient conditions, the exhaust-gas temperature was also sensed by 4 high-response-rate thermocouples located 2 inches radially inward from the wall at 90° intervals immediately downstream of the tailcone.

Recorders. - A multichannel oscillograph was used to record all temperatures and engine speed simultaneously during transient engine operation as well as during steady state at idle and rated speeds. A strip-chart electronic potentiometer was used to record consecutively all temperatures during steady state. The strip-chart record was used to calibrate the oscillograms.

Instrumentation for Strain Survey

Strain gages. - The strain gages were individually made by the pressure-stabilized grid method described in reference 7. Brimor U529, distributed by Morganite, Inc., Long Island, N. Y., was used to cement the gages to the outside of the liner. The gages were located on the surface nearest the engine shaft to correspond with the thermocouples and to avoid the longitudinal weld in the liner. A strain-gage filament of 0.001-inch Karma wire was wound on a jig to form a grid 1/4-inch wide and 3/8-inch long. The grid was pressed to flatten the wire about 10 percent in order to stabilize it dimensionally and thus facilitate handling it during mounting. The grid was then transferred to the liner at a location that had been sprayed with a thin precoat of cement and oriented so as to measure hoop strain (fig. 2(a)). Tube-tipped leads of 0.012-inch Karma wire 1/8-inch long were attached to the ends of the filament. A second coat of Brimor U529 was applied by camel's-hair brush to cement the grid and leads. The tube leads were spotwelded to secondary lead wires of 0.012-inch Karma. These wires were encased in an Inconel conduit swaged for firm support of the wires by the magnesium oxide insulation. The conduit had been secured to the liner by spot-welded Inconel ribbon. A third coat of cement was then used to secure the junction of the secondary leads. Each cement coat was cured at 600° F.

These high-temperature strain gages were mounted at duplicate locations (fig. 2(b)); that is, two gages were located between air-intake holes, two among the cooling louvers, and two near the open end away from geometrical discontinuities.

Circuitry and recorder. - A separate and complete direct-current potentiometer circuit was used with each of the six strain gages. The signals from the gages were amplified and recorded on a 5-channel magnetic-tape recorder. A standard frequency signal and the speed signal from a tachometer generator on the engine were also recorded simultaneously on the 1/2-inch tape.

TEST PROCEDURE

Each day of test operation, the engine was first operated at rated speed of 7950 rpm, and the jet nozzle was adjusted until the exhaust-gas temperature stabilized at 1260° F as indicated by the average of the 14 Chromel-Alumel thermocouples. Subsequent operation was for recording temperature or strain data.

Temperature Survey

The multichannel oscillograph recorded a reference trace, a speed trace, and thermocouple traces during the following time intervals: (1) before starting the engine, (2) during the start, (3) at idle, (4) during acceleration, (5) at rated, and (6) during deceleration. The strip chart recorded temperatures during steady-state conditions at 0, 3000, and 7950 rpm as references for converting trace deflections to temperatures during all conditions of engine operation.

Normal start. - The metal-temperature distribution was determined during the following starting procedure:

(1) The starter was energized, and the rotor speed was increased to about 600 rpm.

(2) The throttle lever was advanced to the starting position indicated on the quadrant.

(3) The ignition system was energized.

(4) The fuel-supply valve was opened.

(5) Ignition occurred.

(6) The engine accelerated slowly to 2000 rpm.

(7) The starter motor was de-energized, and the acceleration continued to idle speed of 3000 rpm.

During steps (5) to (7) the operator observed the exhaust-gas temperature and retarded the throttle to prevent excursions of gas temperatures above about 1600° F, which is the normal temperature limit for service operation of this engine. Control was manual during starting. The fuel regulator operated only above 3000 rpm.

After operation for 2 minutes at idle, the engine was shut down by closing the stopcock valve.

<u>Hot start</u>. - In order to measure the influence of accidental high-temperature starts, metal temperatures were recorded while the engine was operated by using the normal start procedure with the following exception in step (2): The throttle level was advanced beyond the normal starting position marked on the quadrant.

During steps (5) to (7) of the starting procedure the operator retarded the throttle only when the gas temperature threatened to exceed about 2100° F.

<u>Accelerations</u>. - Following a normal start as described previously, the engine was operated at idle for 2 minutes to stabilize temperatures. Acceleration to rated speed was then accomplished by rapidly advancing the throttle and allowing the fuel regulator to control the engine automatically.

In one series of tests deceleration was direct to shut down. In the other series, deceleration was interrupted at idle speed, which was maintained for 2 minutes.

Strain Survey

Magnetic tape was used to record simultaneously the dynamic-strain signals from three strain gages, a standard frequency signal of 400 cycles per second, and the signal from a tachometer generator on the engine shaft, between idle and rated speed conditions. The standard signal was used to check the nominal tape speed of 30 inches per second. Because of the availability of only three channels of the tape recorder for strain signals, it was necessary to repeat the tests after the remaining three strain gages were substituted.

<u>Engine operation</u>. - The normal start procedure described in the previous section was followed to attain idle conditions. The magnetic-tape recorder was then operated during continuous acceleration of the engine. Acceleration between idle and rated speeds was accomplished in $7\frac{1}{2}$ minutes (i.e., 1000 rpm per $1\frac{1}{2}$ min) to permit resonant vibrations to attain maximum amplitudes. Deceleration between rated and idle speeds was also investigated to check the possibility of nonlinear resonances.

DATA REDUCTION

Temperature Survey

Trace deflections on the oscillogram were converted to temperatures by correlation with the steady-state measurements made with a strip chart before starting and during idle and rated speeds. The speed trace was calibrated by recording at intervals of 1000 rpm as determined by a chronometric tachometer.

Within the several speed ranges, the time reference was either ignition or start of acceleration or deceleration. Each reference was indicated by a sudden shift in the trace for the exhaust-gas temperature.

Strain Survey

Each strain-gage signal was analyzed with the aid of an electronic voltmeter, electronic counter, oscillator, and oscilloscope while the magnetic-tape record was played back at a speed of 30 inches per second (as checked by the standard frequency signal). Peak resonance points indicated by the voltmeter were played back several times to determine the engine speed with the counter. The frequency of the vibration at each peak was found by beating an oscillator signal with the strain signal to form a lissajous circle on the oscilloscope screen. The frequency of the oscillator was then measured by feeding the oscillator signal into the counter.

The strain range at each peak was calculated by the equation

$$e = 2.83 \left(\frac{(R + G)^2}{RGKE}\right) V_{rms}$$

where

e strain range

R dropping resistance, ohms

G strain-gage resistance, ohms

K gage factor

E battery voltage, volts

V_{rms} strain-gage signal, volts, root-mean-square

Appropriate correction was made to K for temperature and to V_{rms} for frequency response of the recording system to standard sine wave input.

The strain range that appears in the results is the measured dynamic strain. For the discussion of fatigue strength of the sheet-metal liner, the "apparent stress range" was calculated as the product of strain range and dynamic modulus of elasticity (at the measured metal temperature). This simple conversion was made to give some measure of the magnitude of the total stress. Actually, a biaxial stress state exists in the liner, and a strain-gage rosette would be required to completely describe the stress condition.

RESULTS AND DISCUSSION

Temperature Survey

Preliminary measurements. - Figure 3 shows typical results on two sides of a liner after exposure of the coating of temperature-sensitive paint to rated engine operating conditions for 10 minutes. In order to interpret color changes in the black and white photograph, the areas of different color were separated by black lines and were labeled. The metal temperatures on the side of the liner towards the engine shaft (fig. 3(a)) were generally between 915° and 1065° F (yellow) except for the cooling louvers, which were about 770° F (brown). The temperatures on the side away from the shaft (fig. 3(b)) were generally about 770° F (brown) except for the strips along the air-intake holes, which were between 915° and 1065° F (yellow). At the outlet end, metal temperatures were between 1065° and 1470° F (orange) on all sides. On the basis of these measurements, thermocouples were attached to the shaft side in order to evaluate peak metal temperatures and gradients.

Final measurements. - Variations of metal temperatures (as determined by thermocouples) with time are shown in figures 4 to 7 for the four engine operating conditions considered. The time scale is referenced to ignition for the interval from start to idle, and to the start of acceleration for the transient conditions. Exhaust-gas-temperature and engine-speed curves are also included. In all of these figures the top and middle sets of curves were derived from the same engine test. (Note that the exhaust-gas-temperature curves and the speed curves are identical for these two plots.) Two sets of axes were used to avoid confusion among the curves. The bottom sets of curves were derived from another test, with the same operating conditions, because the instrumentation could not handle all the thermocouples simultaneously. (Note that the exhaust-gas-temperature and speed curves for this set of axes are not exactly the same as the other two.) Duplicate tests were run in both cases, and the curves shown are typical.

Normal and hot starts. - From the comparison of metal temperatures in figures 4 and 5, it can be seen that the transient influence of the hot gas is not felt at the thermocouple locations. The liner is apparently sufficiently cooled even during the hot start; that is, the hot core produced by the burning of the rich fuel mixture is separated from the liner walls by a layer of cooling air and does not affect the liner at the thermocouple locations.

Accelerations to rated speed and decelerations. - Between idle and rated speeds, the curves of figures 6 (interrupted shutdown) and 7 (uninterrupted shutdown) are consistent. Except for the gas temperature, the deceleration curves of figure 6 closely resemble the combined curves of figure 7. In other words, the two conditions of shutdown cannot be distinguished at the liner wall.

During preliminary tests, several slow accelerations to rated were made with a duration of $1\frac{1}{2}$ minutes, as compared with about 30 seconds for the tests reported, but no appreciable difference in peak metal temperatures was measured.

Thermal gradients. - The thermal gradients at each side of two cooling louvers are plotted against time in figure 8 for three of the four engine operating conditions. No plot is presented for the hot start because it is very nearly the same as for the normal start, as previously discussed. The gradients were computed by subtracting the metal temperature nearest the edge of the louver from that between louvers and dividing by the thermocouple spacing (3/8 in.). A negative gradient, therefore, merely indicates that the temperature nearest the louver was higher.

In figures 8(a) and (c) only three curves are plotted because no signal was received from one thermocouple next to a louver. All four curves are plotted in figure 8(b) because all thermocouples concerned performed satisfactorily.

In general, the gradients are less than 300° F per inch throughout the engine operating conditions. Because the thermal gradients measured during hot starts are no more severe than for normal starts, it would be expected that repeated hot starts would not reduce the service life of liners. For the two tests to rated speed (figs. 8(b) and (c)), the gradients near one louver increase rapidly above 5000 rpm and reach a peak value of about 1500° F per inch at maximum speed and then remain at about 1100° F per inch during steady state. In figure 8(b), one gradient increases rapidly during the normal start and reaches a peak of 800° F per inch at 2500 rpm. It remains somewhat uniform throughout the acceleration to rated and deceleration to idle. (The corresponding gradient is not shown in figure 8(c) because of the failure of one thermocouple.) In view of the high gradients and the stress concentrations at the sharp edges of the louvers, it seems that repeated accelerations to rated speed could be a major contributor to the cracks that are experienced in service combustor liners.

Distributions of metal temperatures in the circumferential direction. - The distributions shown in figure 9 are for steady-state conditions at idle and rated speeds. These curves are typical of the temperature distributions that existed at intermediate speeds. The metal temperatures are nearly uniform at idle except for the points at both ends of the curves, located at air-intake holes. If the fuel spray were uniform, the metal temperature at the middle pair of holes would be the same as the end points, or at least higher than its immediate neighbors. A somewhat lower temperature at the middle might be explained by the fact that the air-intake hole just upstream of this thermocouple is not plunged and is larger than the others (1-in. diam. against 3/4-in. diam.) to accommodate a water-injection orifice, and thus will admit more cooling air when the injection apparatus is not installed.

Metal temperatures nearest the edges of louvers were expected to be less than between louvers. Such is the case at one louver at rated speed, but the reverse occurred at the other. In general, such inconsistencies result from nonuniform burning of fuel. Similar results were measured in a J33 (ref. 1). The slightly lower metal temperatures during final idle speed were obviously caused by the lower gas temperature.

Strain Survey

Vibratory modes. - Cylinders with radius-to-thickness ratios of the order of those encountered in combustor liners are primarily susceptible to curved-plate type of vibrations rather than to beam modes. The plate type of vibrations can be considered to be composed essentially of three types of normal modes: (1) those having nodes that run parallel to the longitudinal axis of the cylinder, (2) those having nodes that are circumferential, and (3) those having both longitudinal and circumferential nodes. In the third type, the number of nodes in the longitudinal direction can be any value, irrespective of the number of nodes in the circumferential direction. It is also possible for several normal modes having similar frequencies to combine into what are termed "compounded normal modes." These modes have natural frequencies of their own. The curved-plate type of vibrations described herein are analogous to the flat-plate modes described in reference 6. The vibratory modes of the actual combustor liners would be expected to react much the same as described herein for the continuous cylinders, with the exception that the louvers and holes would introduce further complexities.

In the following discussion, the strain data are presented as a "strain range," or complete change in dynamic-strain level. For symmetrical vibration superimposed on a zero static strain, the maximum strain would be one-half of the observed strain range.

Critical-speed diagrams. - The variations with engine speed of the measured dynamic strains and the vibratory frequencies were plotted for all strain-gage locations (fig. 10). These data indicate that the combustor liner was susceptible to vibration which caused a strain range between 50 and 190 microinches per inch throughout the range of frequencies from about 4000 to 10,500 cycles per second. Each pair of data points represents a peak amplitude of vibration; that is, each point plotted as a strain range has a corresponding frequency plotted below for the same engine speed (see DATA REDUCTION, Strain Survey, p. 8).

The data from individual strain gages were replotted and grouped for geometrically similar locations. The dynamic strains and frequencies measured between cooling louvers are shown in figure 11; between air-intake holes, in figure 12; and near the combustor outlet, in figure 13.

The large number of data points (fig. 10) appears to verify the assumption that the liner would be subjected predominantly to plate-type vibrations with the accompanying large number of vibrational modes. Figures 11, 12, and 13 indicate that each strain gage measured vibrations throughout the range of frequencies. Although most of the points lie along the 79th order line of engine speed, an appreciable number of points are on the 78th and 76th order lines. The vibratory frequencies were independent of strain-gage location. The sheet-metal liner vibrates at the same frequencies (with respect to engine speed) between the small cooling louvers (fig. 11) and large air-intake holes (fig. 12) as it does in the relatively continuous structure near the combustor outlet (fig. 13). This indicates that the liner is vibrating as an integral unit rather than as more or less isolated panels between louvers and holes. No significant differences were noted in the data obtained during increasing and decreasing speeds; this indicates the absence of nonlinear resonances.

Sources of excitation. - The primary source of excitation of the liner is attributed to the 12th (last) and 9th compressor rotor stages, which are comprised of 79 blades each. The 11th and 8th rotor stages consist of 76 blades each and apparently contribute the secondary excitations at the higher engine speeds (above 5000 rpm). Other resonances are obviously excited by the 78 blades in the 10th rotor stage. The stator stages (table I) were not expected to excite the liners because they are stationary relative to the combustor.

Dynamic strains. - The strain data corresponding to the measured frequencies show considerable scatter throughout the speed range between idle and rated. No trend is apparent except that strain range generally decreased as frequency increased and was uniform at the higher speeds. The largest strains were measured between air-intake holes (fig. 10) over a range of frequencies from about 4000 to 7000 cycles per second.

All of the air-intake holes were 3/4-inch diameter (with a plunged reinforcement on the downstream side) except for four holes 1 inch in diameter (without reinforcement) equally spaced around the middle; these 1-inch holes accommodate water-injection nozzles. Peak values of dynamic-strain range should be expected at these locations on both sides of the 1-inch-diameter hole. The maximum dynamic-strain range measured in the circumferential direction was 190 microinches per inch and occurred between air-intake holes (fig. 12(a)). Actually, this value of strain results from an integration of strain over the area covered by the strain gage. This strain corresponds to an apparent stress range of about 5400 psi. This calculation of apparent stress range considered the variation of dynamic modulus of elasticity with temperature and assumed a uniaxial stress state. The temperatures at the strain gages were assumed to be adequately defined by the metal temperatures measured in the other liner.

The maximum apparent dynamic stress measured away from the edge of a louver was about ± 2700 psi. The stress at the edge of a louver would be higher because of the stress concentration caused by the sharp notch. The endurance limit for Inconel is reported to be 26,500 psi at 1170° F, but this value was obtained for smooth bars at 10^8 cycles of reversed bending. No data are available for Inconel sheet, but other investigations indicate that the endurance limit would be less for sheet than for bars. In addition, sheet materials are very notch-sensitive at elevated temperatures. The frequent cracking of liners at the sharp edges of louvers is a consequence of this.

At the high frequencies measured, a sheet-metal liner accumulates 10^8 cycles in about 3 hours of operation at rated speed. Fatigue data are customarily confined to 10^8 cycles, and it is possible that the fatigue strength of sheet would be appreciably lower at 10^9 cycles.

In summary, the applicable endurance limit would be the value of 26,500 psi (for smooth bars at 1170° F) with suitable adjustment made for (1) sheet material, (2) stress concentration due to sharp notches, (3) high vibratory frequencies that result in rapid accumulation of cycles of stress, (4) stress corrosion effects, and (5) other loads. In the absence of a basis for evaluating these corrections, it should be pointed out that the final value of endurance limit might conceivably approach the maximum stresses in the liner tested. It appears, therefore, that mechanical fatigue might contribute measurably to cracking of a tubular liner of the type tested.

Method for reducing vibratory strains. - Although cracks in sheet-metal liners result from a combination of loadings (see REMARKS ON GENERAL STRESS STATE IN LINER, p. 2), the service life of a liner would be expected to be increased by the reduction of any one of the contributing loads. On the basis of the results of other investigators on methods for reducing stresses in turbine rotor blades (ref. 8), it is likely that a modified spacing arrangement of the blades in at least the last two compressor rotor stages would reduce the vibratory stress in the liner to a considerable extent. By modifying the rotor stages, the liner would be excited at additional orders of engine speed, but at a lower amplitude.

SUMMARY OF RESULTS

Temperature Survey

The results of temperature measurements made on a liner of a J47-27 turbojet engine during several operating conditions are summarized as follows:

1. The metal temperatures were practically the same during normal and hot starts at thermocouple locations near the midlength of the liner (where cracking usually occurs) as well as near the combustor outlet.

2. Peak metal temperatures were not influenced appreciably by the rate of acceleration to rated speed.

3. Liner walls experienced little difference in thermal gradients near louvers during shutdown, whether or not an interruption in speed was made at idle.

4. The maximum thermal gradient measured was about 1500° F per inch and occurred near a cooling louver at rated speed. This transient value decreased to about 1100° F per inch during steady-state operation.

Strain Survey

During the accelerations between idle and rated speeds, the following results were obtained:

5. The predominant resonances in the liner were of the 79^{th} order of engine speed and were attributed to the 12^{th} (last) and 9^{th} compressor rotor states which consist of 79 blades.

6. Above 5000 rpm, resonances of the 76^{th} order were also observed. This secondary excitation was attributed to the 76 blades in each of the 11^{th} and 8^{th} compressor rotor stages.

7. Resonances of the 78^{th} order were measured throughout the speed range and were caused by the 78 blades in the 10^{th} compressor rotor stage.

8. The liner was susceptible to a range of vibratory frequencies between 4000 and 10,500 cycles per second. These frequencies were found to be independent of strain-gage location which indicated that the liner vibrated as an integral unit.

9. Dynamic-strain measurements showed considerable scatter. The maximum average strain range measured in the circumferential direction was 190 microinches per inch and occurred between air-intake holes.

E-387

10. Mechanical fatigue might contribute measurably to cracking of tubular liners. Although the maximum apparent dynamic-stress range was 5400 psi, it is conceivable that the peak dynamic stress at the edge of a louver might approach the endurance limit for Inconel sheet during the service life of a liner.

CONCLUDING REMARKS

Although this investigation was confined to J47-27 liners, the results are considered to apply to tubular liners in general. Cracking is caused by a combination of loads imposed on the liner during engine operation. If any of the contributing loads were reduced, the service life of the liner would be extended.

On the basis of the results of another investigation on methods for reducing turbine rotor blade stresses, it appears that a modified spacing of the last five compressor rotor stages could be used to reduce the excitation amplitudes and hence the maximum liner vibratory amplitude or stress. Vibrations could also be damped by intermediate supports for the liner.

The influence of thermal stresses could be reduced by providing adequate cooling by the secondary air for all operating conditions, especially severe transients.

The condition of the fuel nozzle has a marked effect on the life of a liner. A nonuniform spray is likely to cause hot spots that could either burn the sheet metal or induce thermal fatigue.

Surface finish of the edges of cutouts and elimination of sharp corners will also increase the reliability of liners.

Lewis Research Center
National Aeronautics and Space Administration
Cleveland, Ohio, October 2, 1959

E-387

REFERENCES

1. Lewis Laboratory Staff: Factors That Affect Operational Reliability of Turbojet Engines. NACA RM E55H02, 1956.

2. Clarke, J. S., and Lardge, H. E.: The Performance and Reliability of Aero-Gas-Turbine Combustion Chambers. Trans. ASME, vol. 80, no. 8, Nov. 1958, pp. 1741-1755.

3. Wilsted, H. D., Duffy, Robert T., and Grey, Ralph E.: Operating Temperatures of I-40-5(J33) Turbojet Engine Burner Liners and the Effect of Temperature Variation on Burner-Liner Service Life. NACA RM E8F29, 1948. (Supersedes NACA MR E6E24.)

4. Calvert, Howard F., Braithwaite, Willis M., and Medeiros, Arthur A.: Rotating-Stall and Rotor-Blade-Vibration Survey of a 13-Stage Axial-Flow Compressor in a Turbojet Engine. NACA RM E54J18, 1955.

5. Morgan, W. C., and Morse, C. R.: Experimental Investigation of the Vibration Characteristics of Four Designs of Turbine Blades and of the Effect Produced by Varying the Axial Spacing Between Nozzle Blades and Turbine Blades. NACA RM E51J25, 1952.

6. Grinsted, B.: Nodal Pattern Analysis. Proc. Instit. Mech. Eng., vol. 166, no. 3, 1952, pp. 309-321; discussion pp. 322-326.

7. Kemp, R. H., Morse, C. R., and Hirschberg, M. H.: Application of a High-Temperature Static Strain Gage to the Measurement of Thermal Stresses in a Turbine Stator Vane. NACA TN 4215, 1958.

8. Kemp, Richard H., Hirschberg, Marvin H., and Morgan, William C.: Theoretical and Experimental Analysis of the Reduction of Rotor Blade Vibration in Turbomachinery Through the Use of Modified Stator Vane Spacing. NACA TN 4373, 1958.

TABLE I. - COMPRESSOR SUBASSEMBLY FOR J47-27

Stage	Number of blades	
	Rotor	Stator
Exit		[a]120
12	79	[a]72
11	76	90
10	78	90
9	79	90
8	76	83
7	58	90
6	56	88
5	54	64
4	52	64
3	50	60
2	48	56
1	41	48

[a]Stator blades at exit and at 12th stage are adjacent.

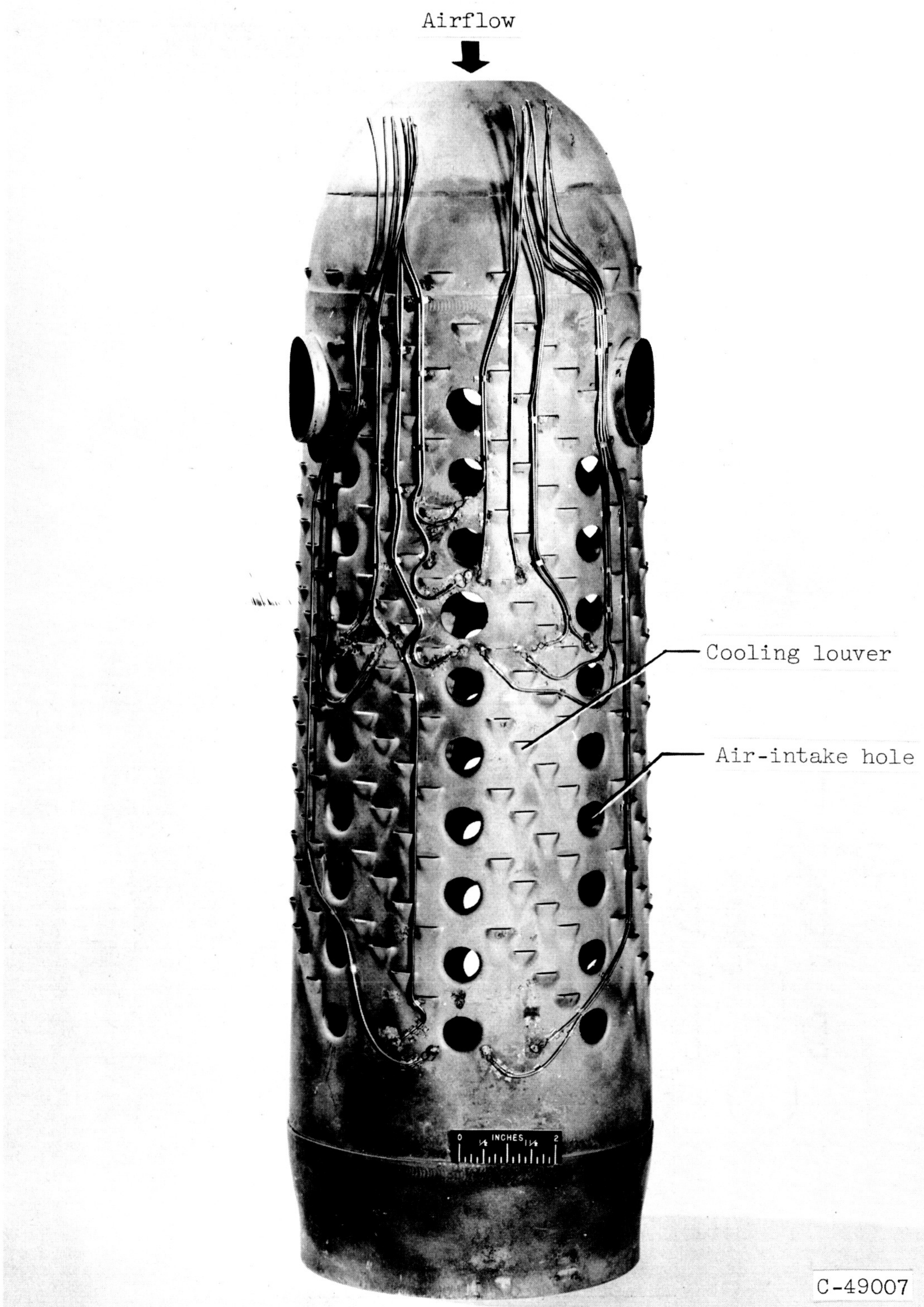

(a) Method of attachment.

Figure 1. - Thermocouple installation on turbojet combustor liner.

E-387

CK-3 back

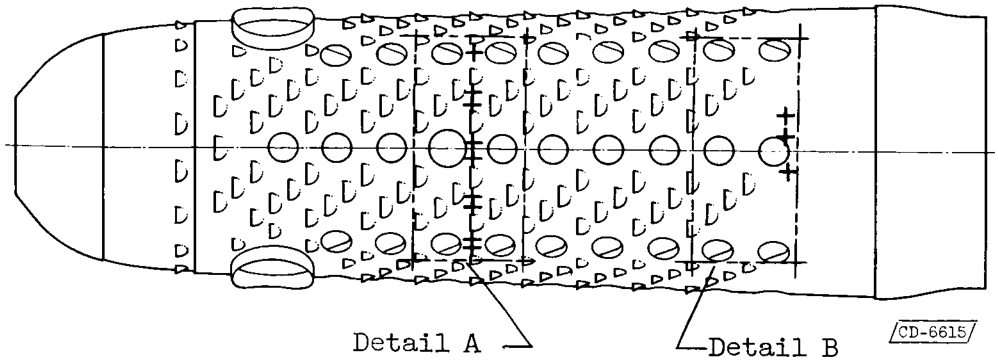

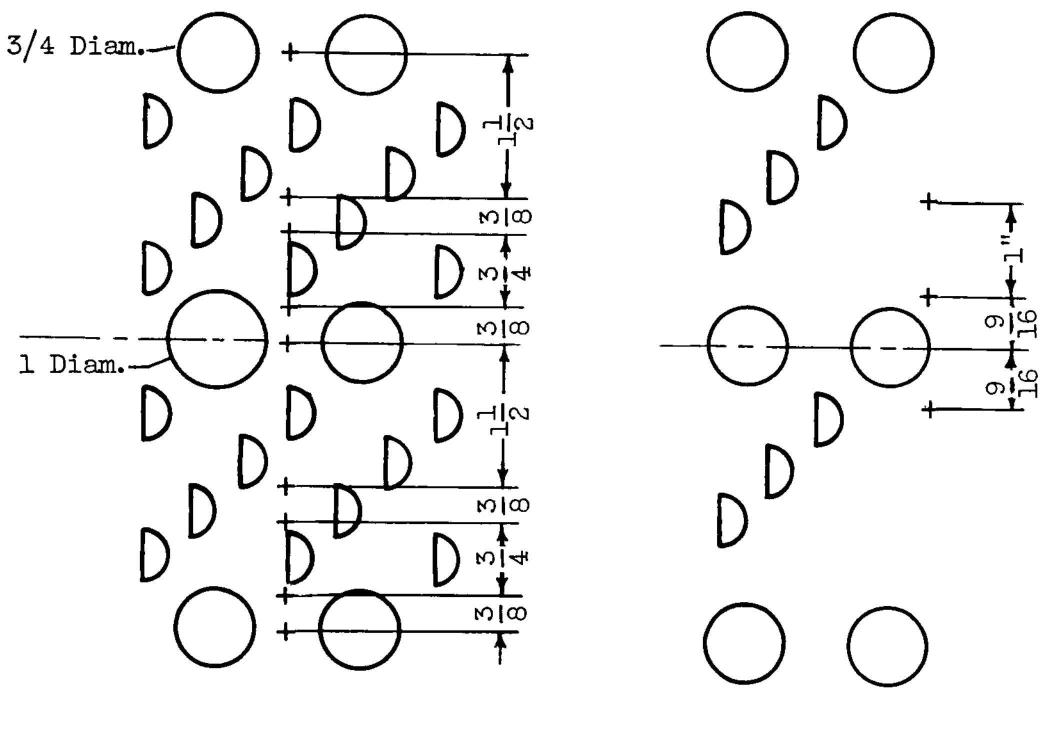

Detail A

Detail B

(b) Locations of thermocouples.

Figure 1. - Concluded. Thermocouple installation on turbojet combustor liner. (All dimensions in inches.)

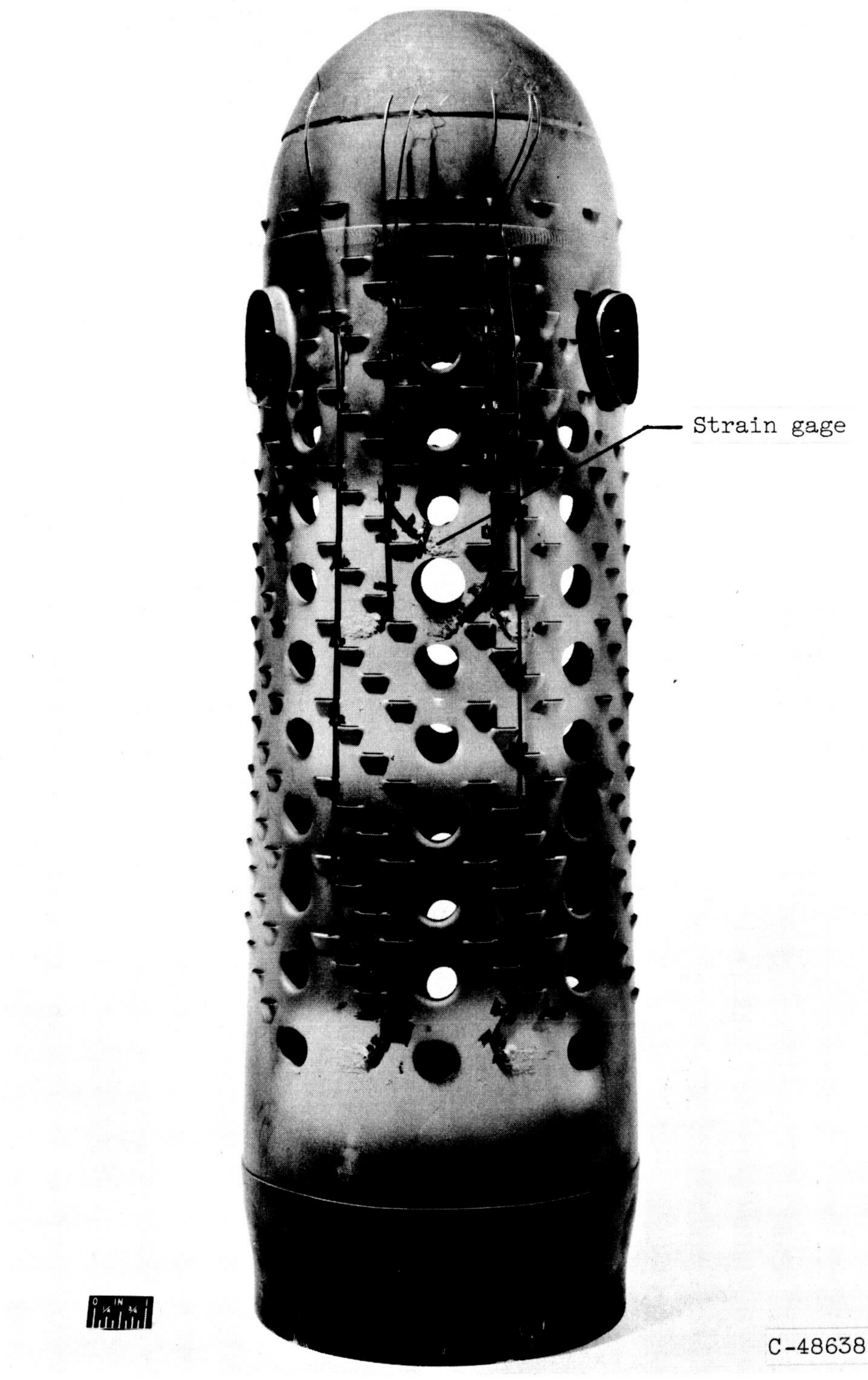

(a) Method of attachment.

Figure 2. - High-temperature strain gages mounted on turbojet combustor liner to measure hoop strains.

E-387

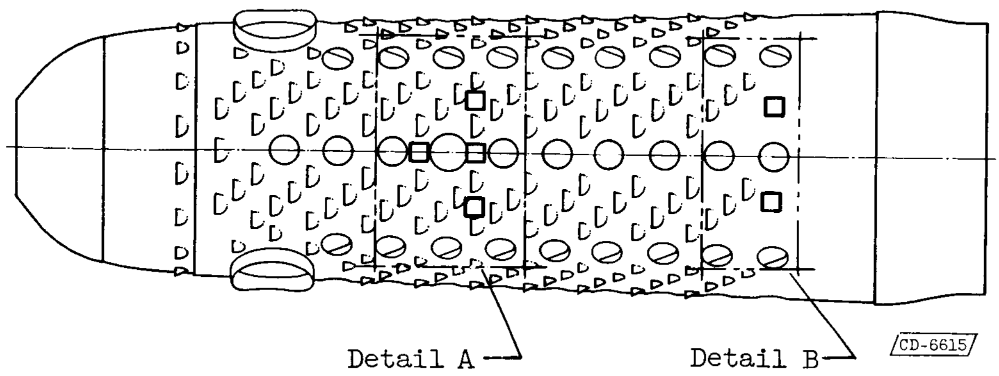

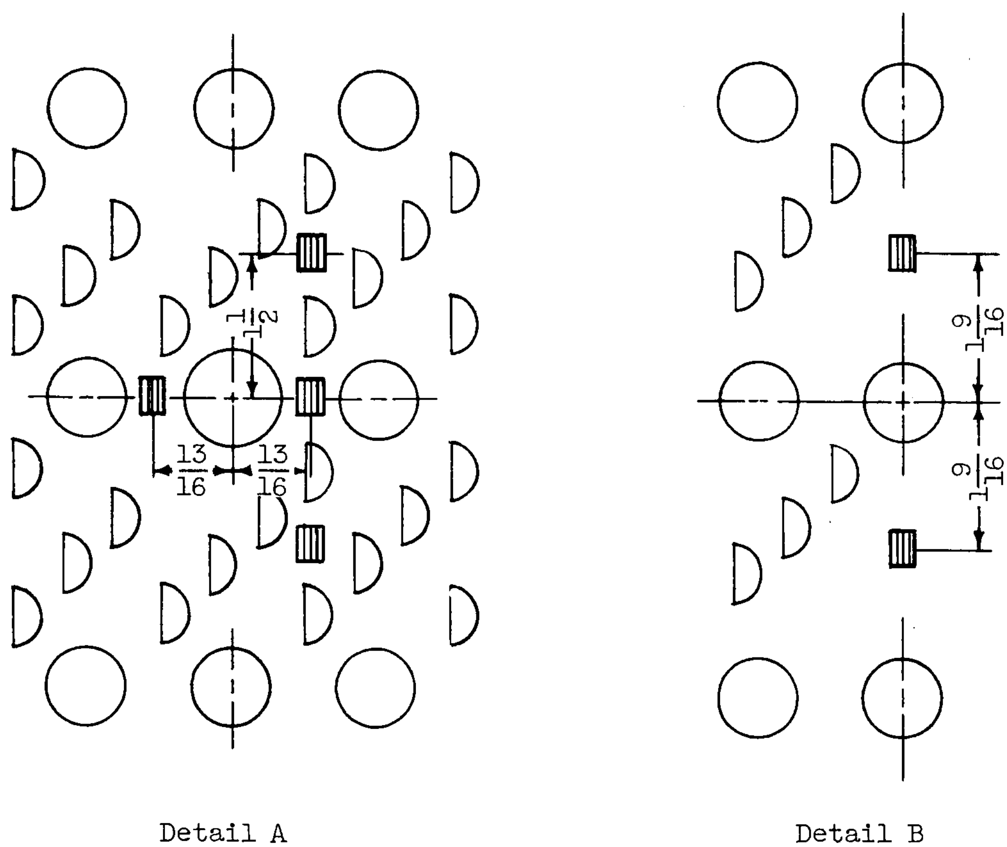

(b) Locations of strain gages.

Figure 2. - Concluded. High-temperature strain gages mounted on turbojet combustor liner to measure hoop strains. (All dimensions in inches.)

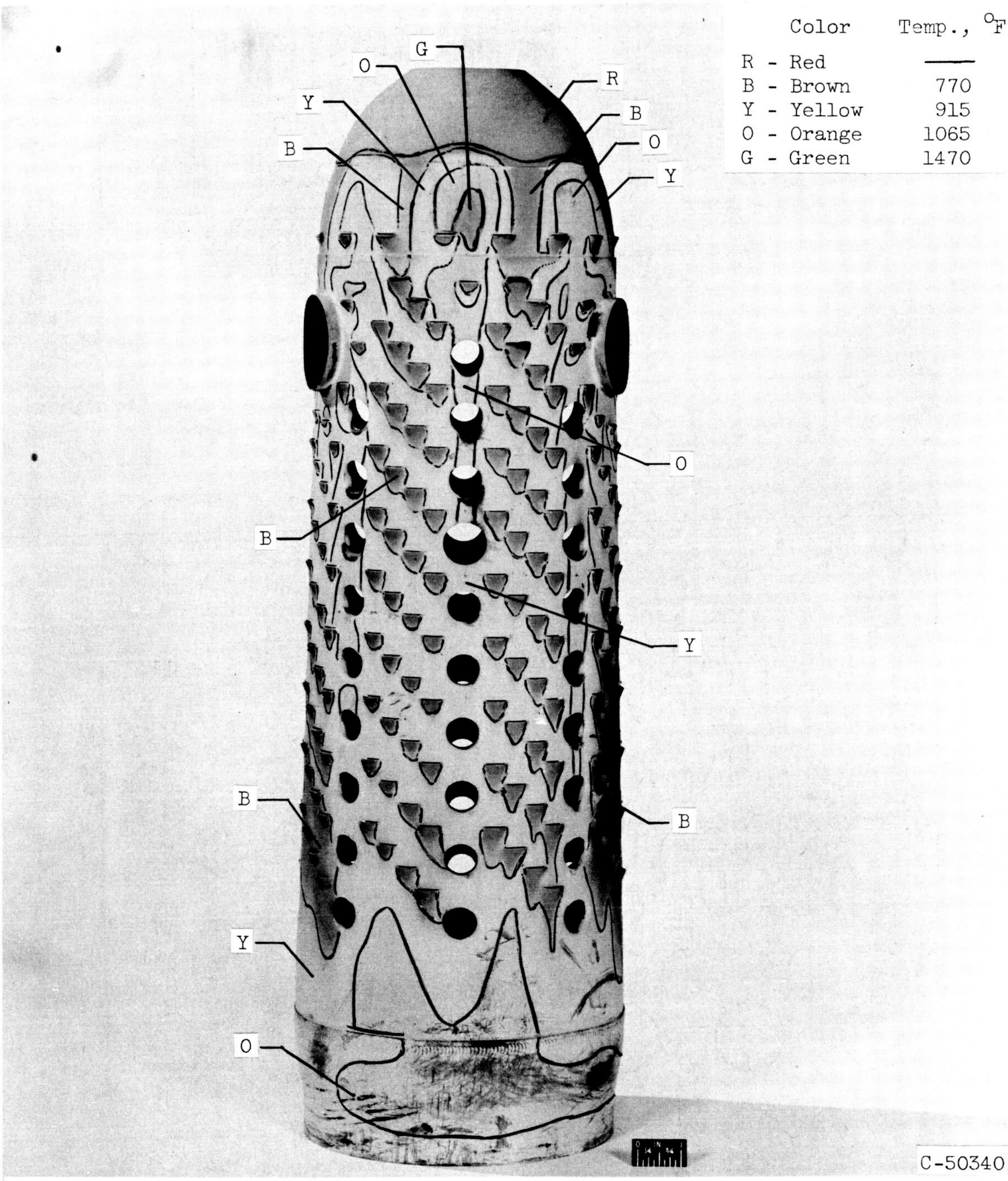

(a) Side towards engine shaft.

Figure 3. - Metal temperatures indicated by temperature-sensitive paint.

E-587

E-387

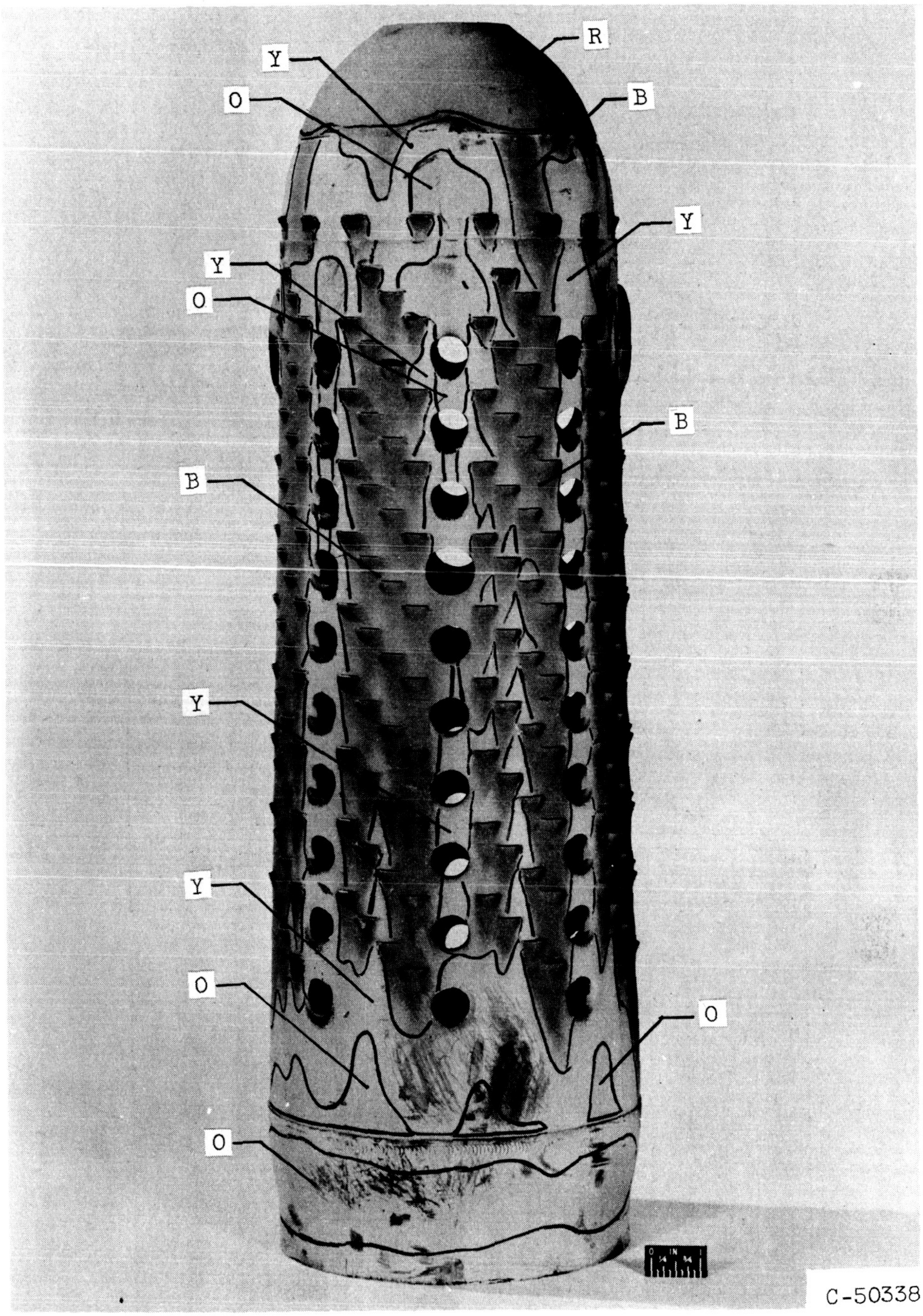

(b) Side away from engine shaft.

Figure 3. - Concluded. Metal temperatures indicated by temperature-sensitive paint.

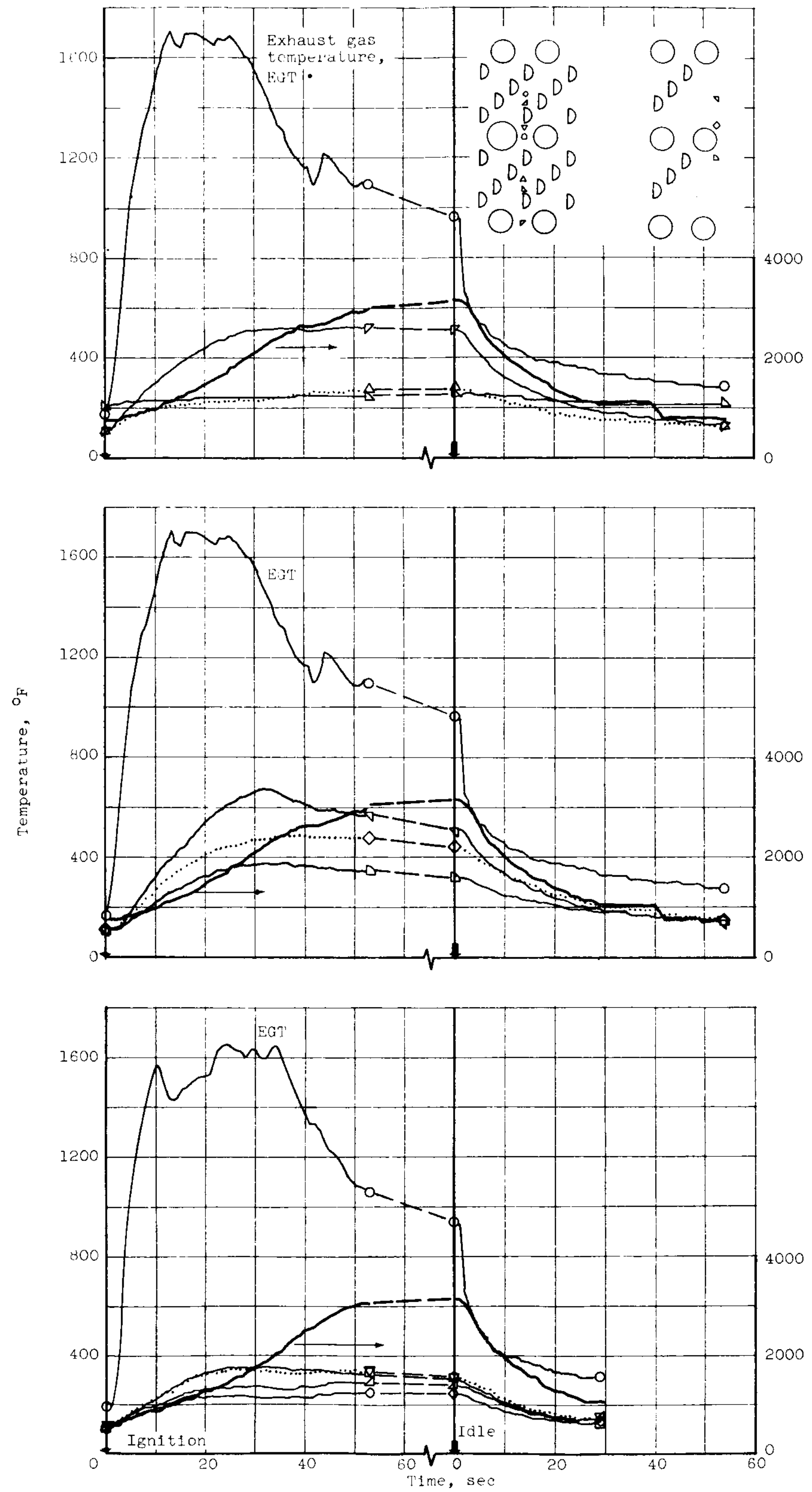

Figure 4. - Temperatures measured in liner during normal start and shutdown.

E-387

E-387

CK-4

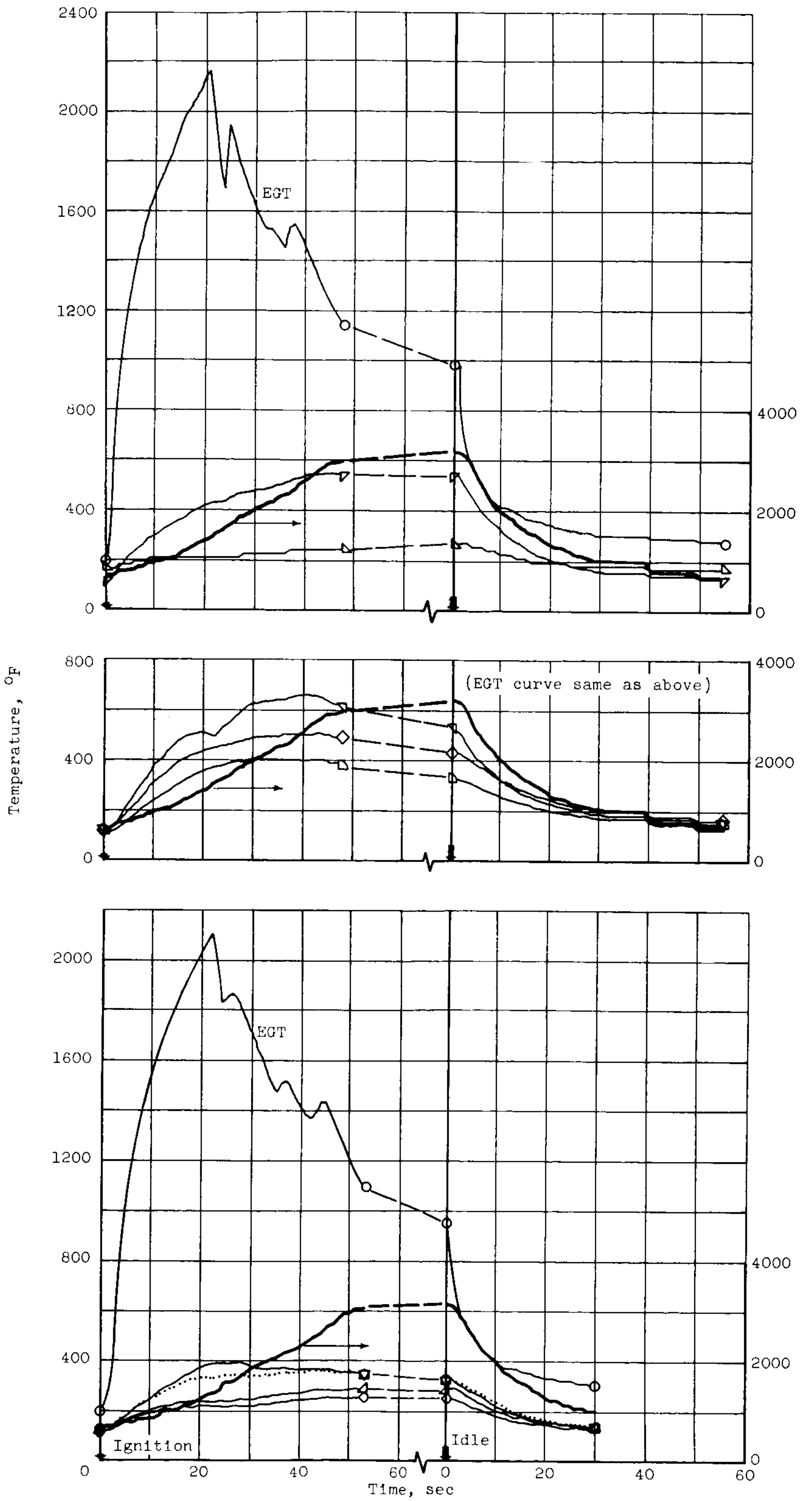

Figure 5. - Temperatures measured in liner during hot start and shutdown.

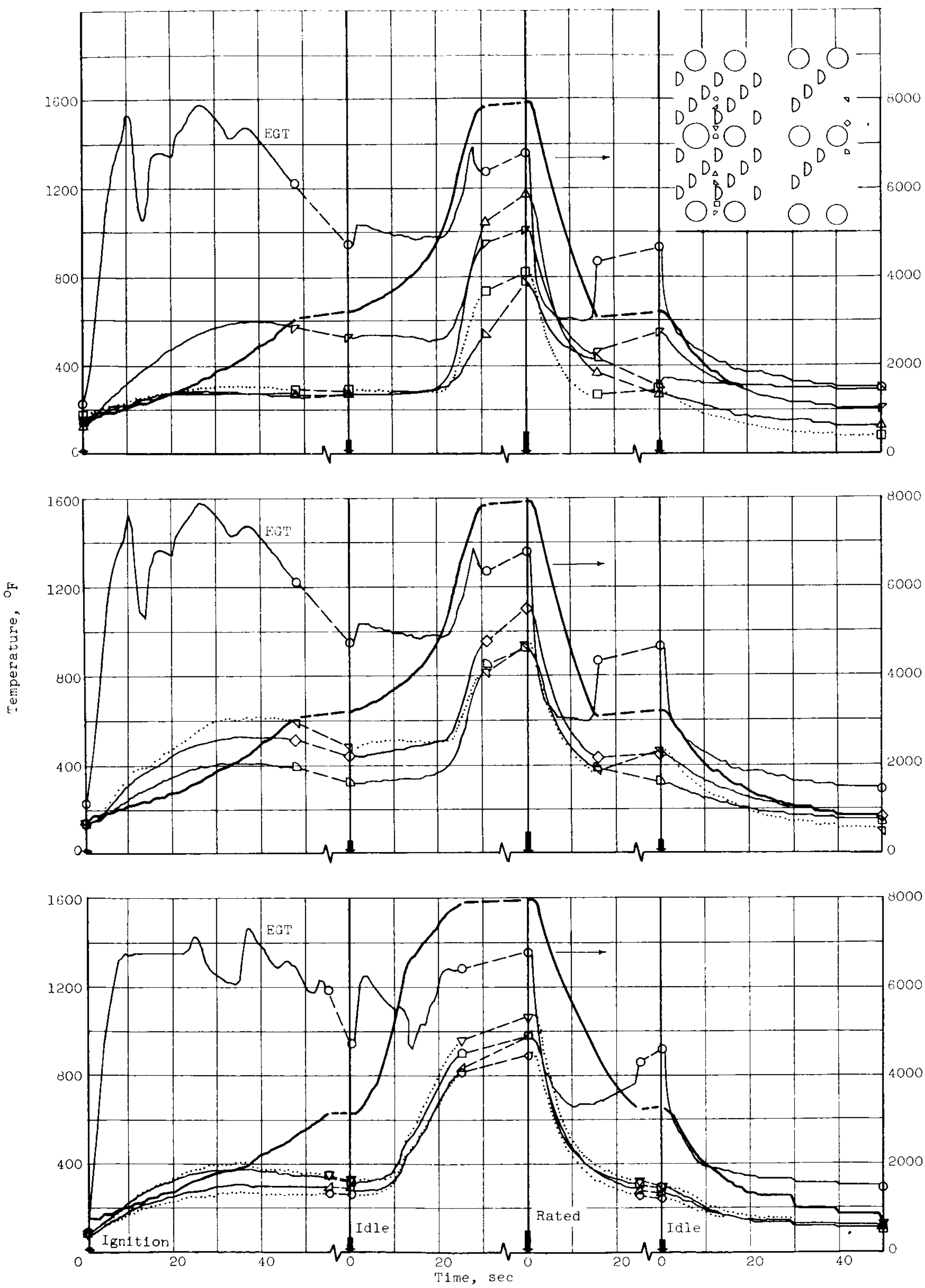

Figure 6. - Temperatures measured in liner during normal start followed by acceleration to rated and shutdown interrupted at idle.

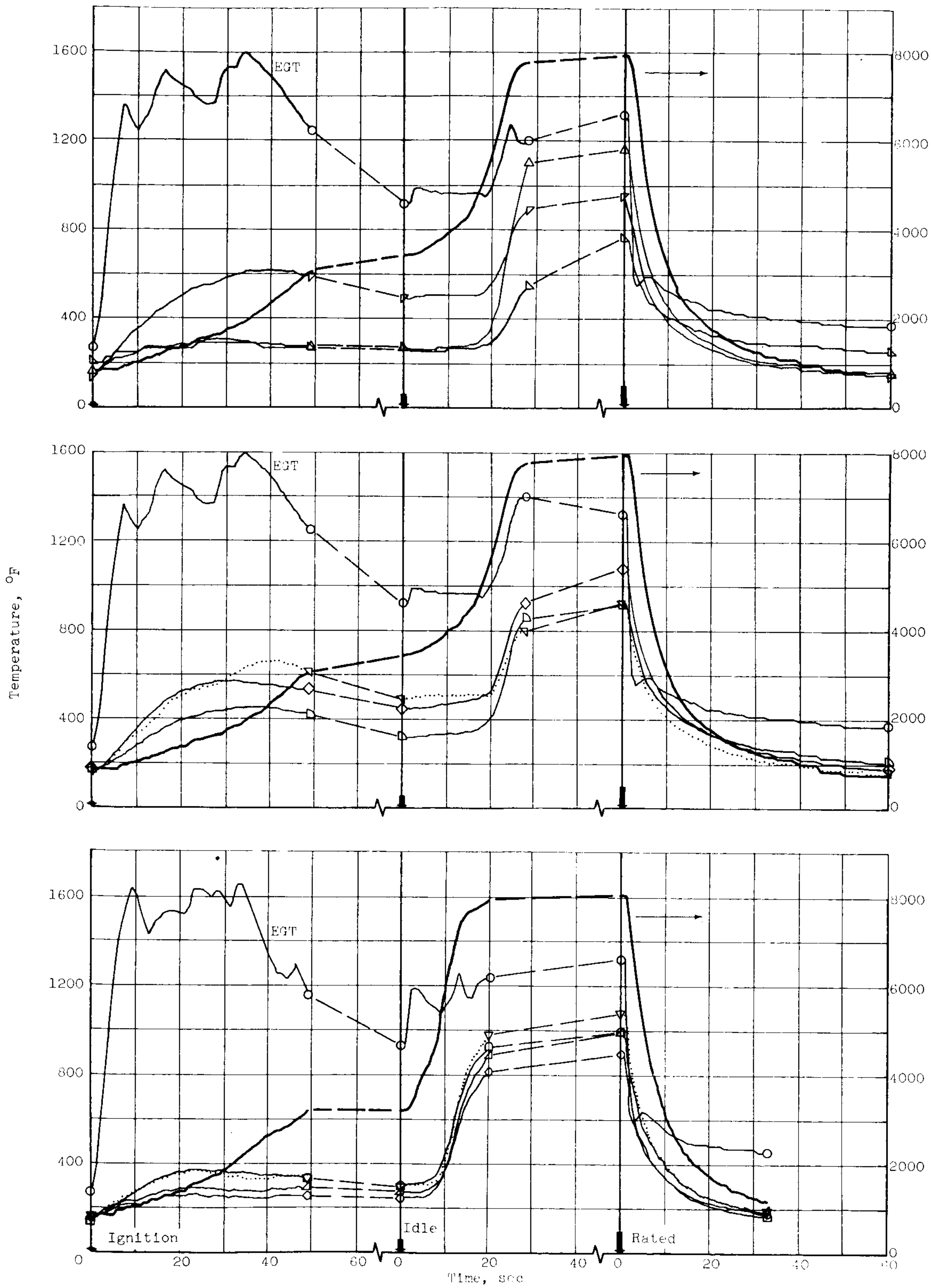

Figure 7. - Temperatures measured in liner during normal start followed by acceleration to rated and uninterrupted shutdown.

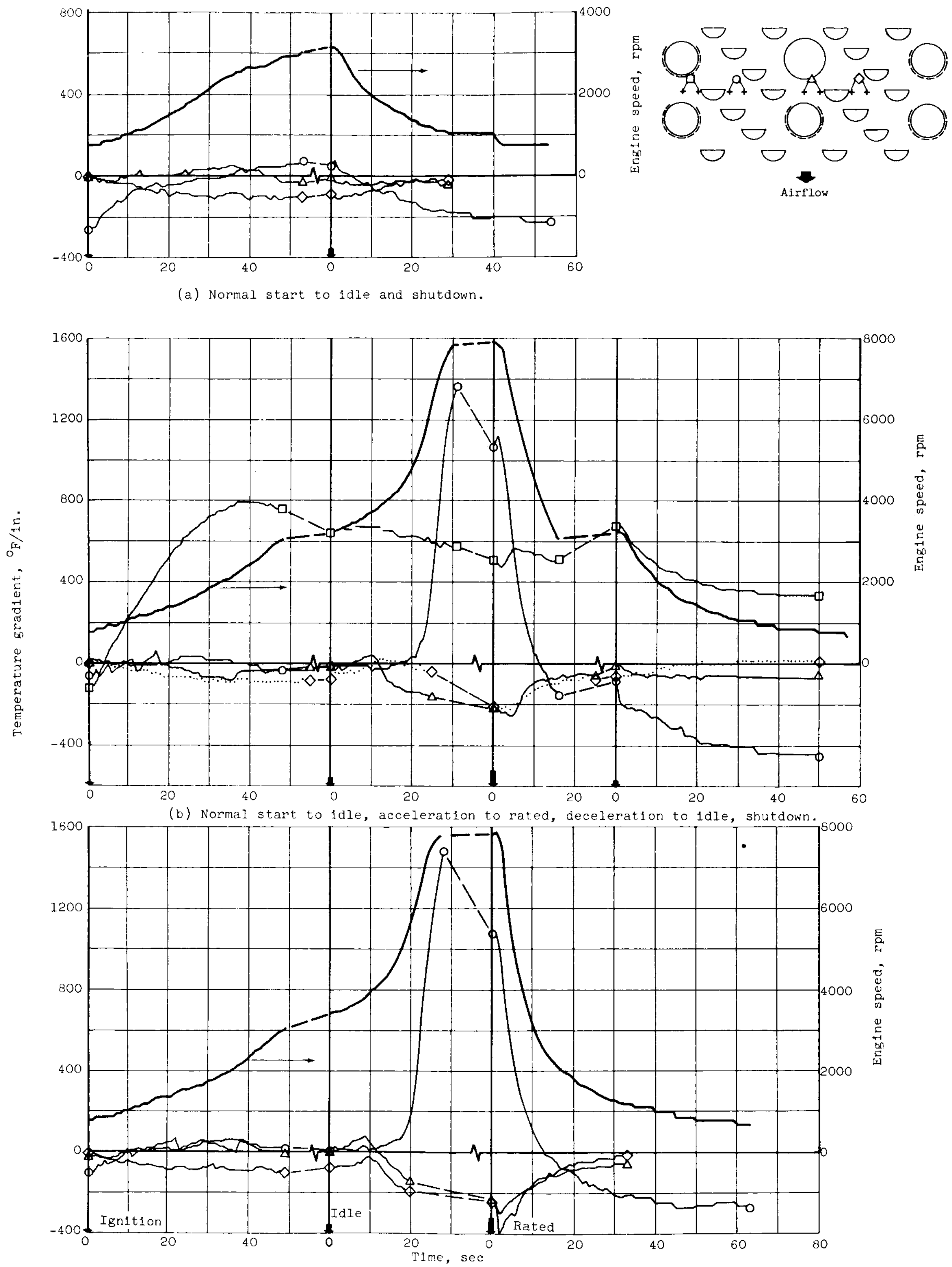

(a) Normal start to idle and shutdown.

(b) Normal start to idle, acceleration to rated, deceleration to idle, shutdown.

(c) Normal start to idle, acceleration to rated, shutdown.

Figure 8. - Thermal gradients in combustor liner near louvers.

E-387

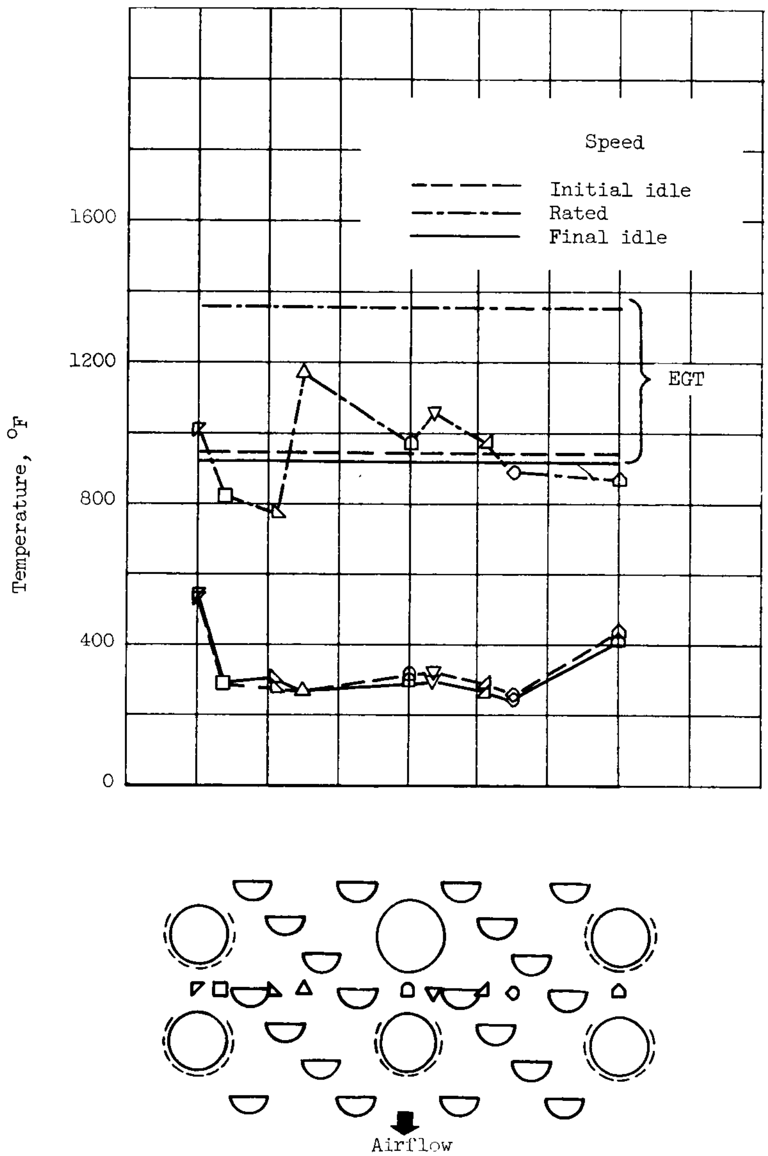

Figure 9. - Distributions of metal temperatures in the circumferential direction during initial idle, rated, and final idle speeds. (Exhaust-gas temperatures also indicated.)

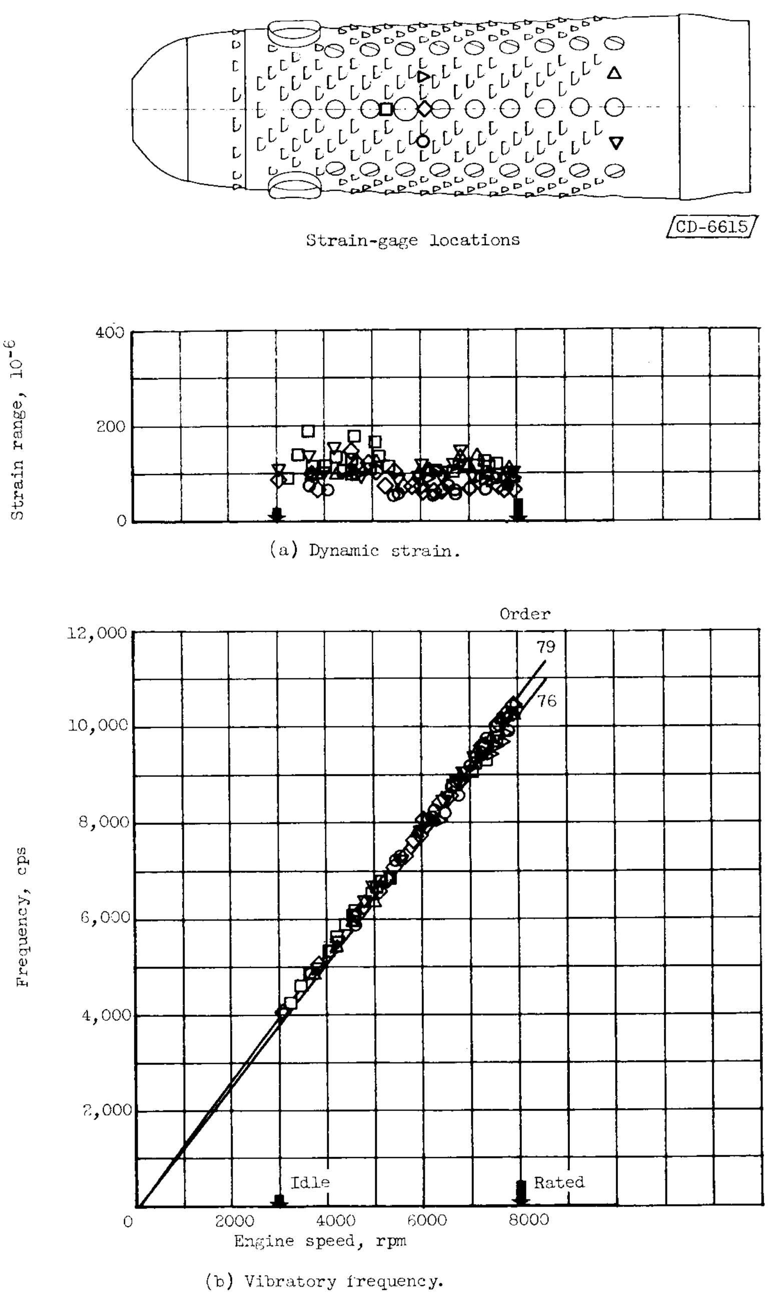

Figure 10. - Critical speed diagram for all strain gages.

E-387

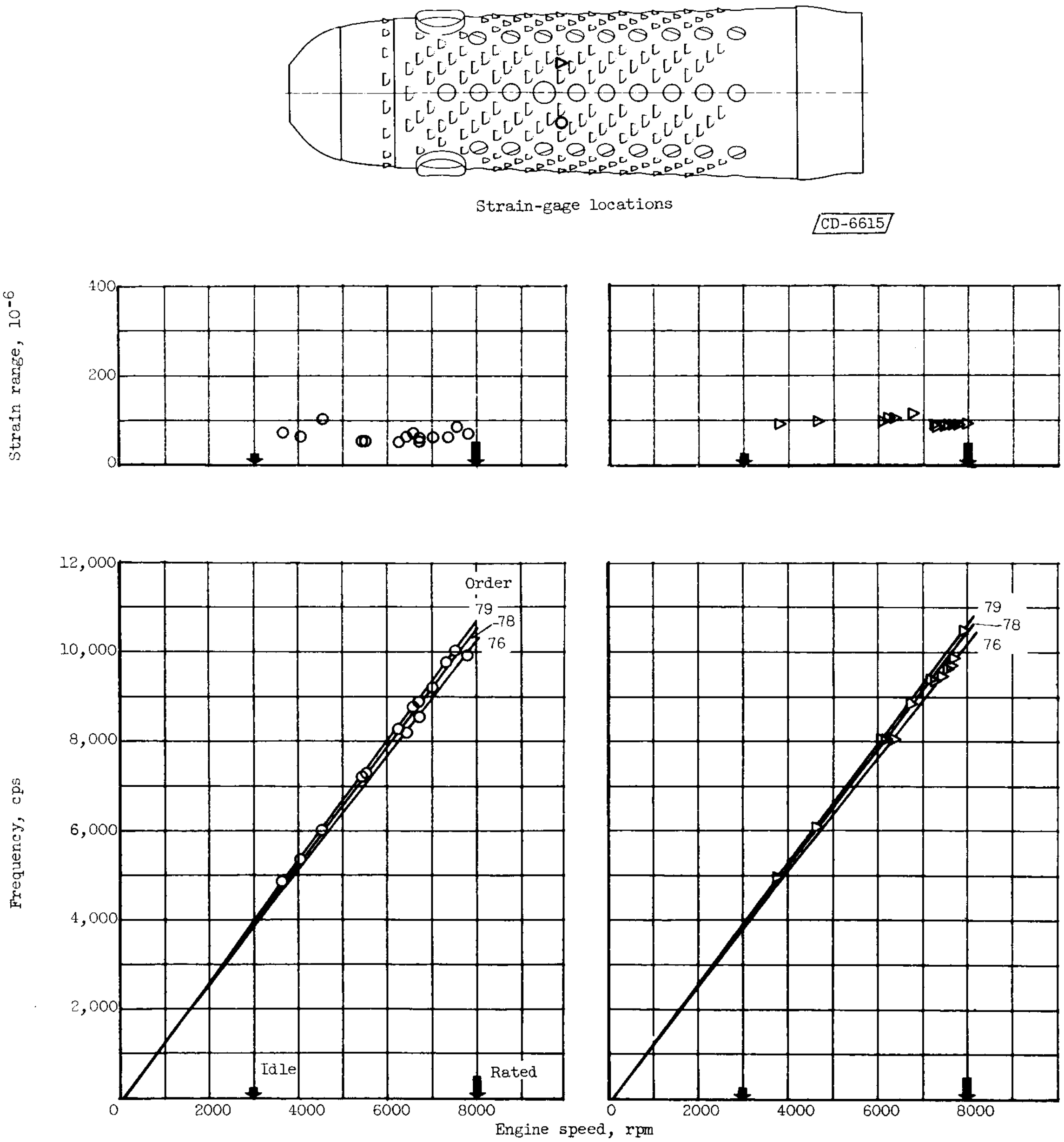

(a) Increasing speed.

(b) Decreasing speed.

Figure 11. - Critical speed diagrams for strain gages at similar locations between louvers.

E-387

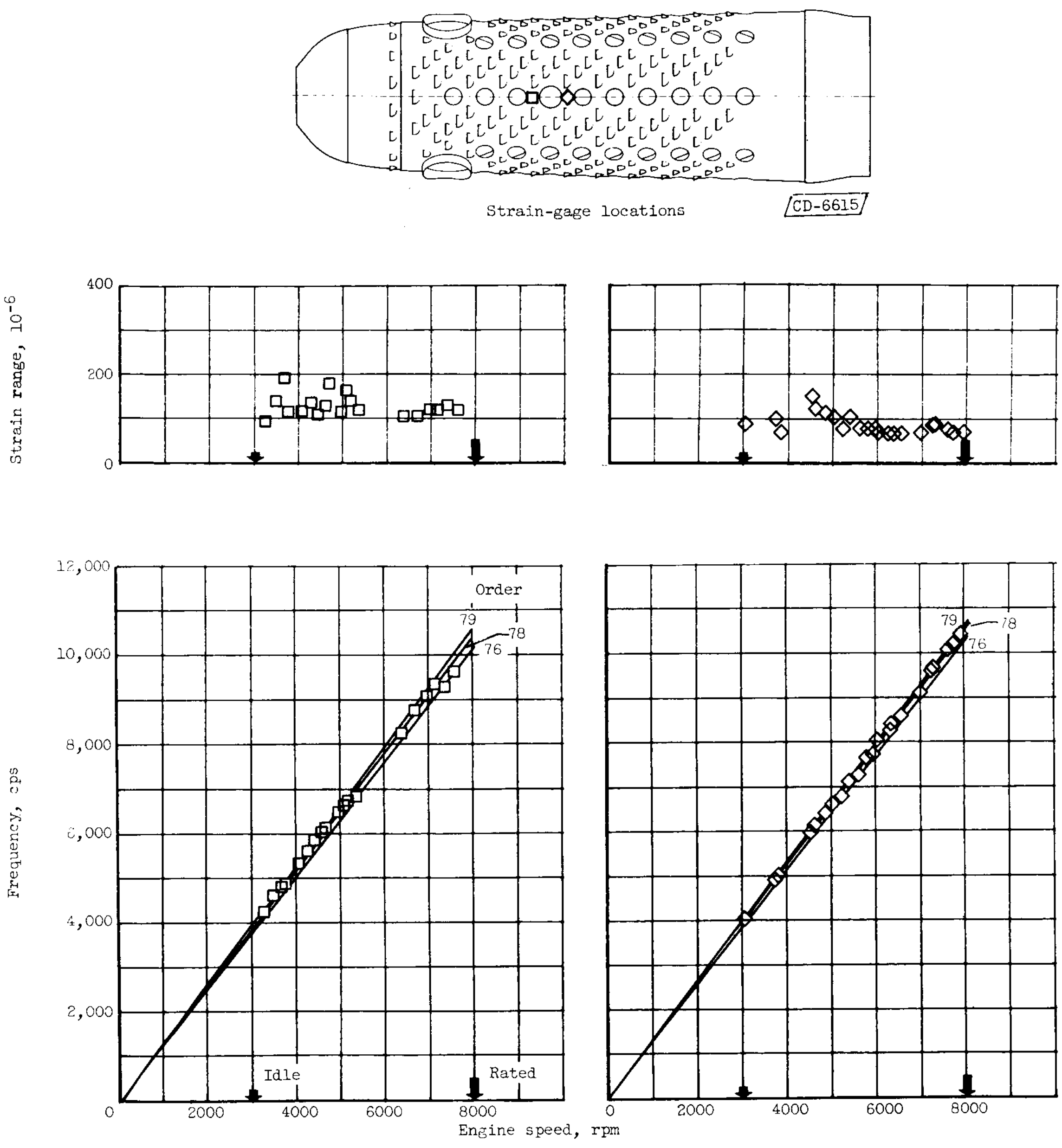

(a) Increasing speed.

(b) Decreasing speed.

Figure 12. - Critical speed diagrams for strain gages at similar locations between air-intake holes.

E-387

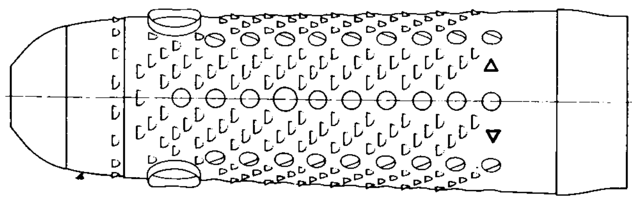

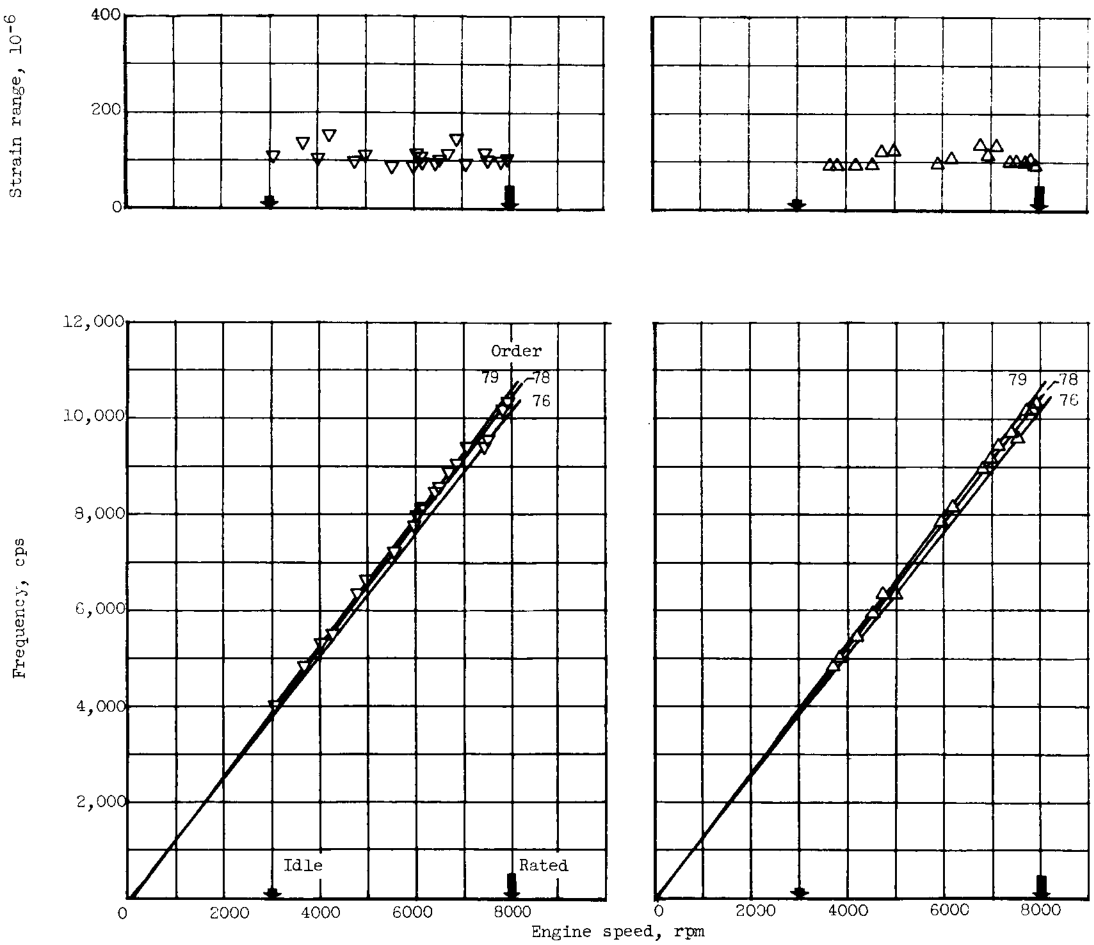

(a) Increasing speed.

(b) Decreasing speed.

Figure 13. - Critical speed diagrams for strain gages at similar locations near combustor outlet.